OPEN ACCESS

Scholars International Journal of Chemistry and Material Sciences

Abbreviated Key Title: Sch Int J Chem Mater Sci
ISSN 2616-8669 (Print) |ISSN 2617-6556 (Online)
Scholars Middle East Publishers, Dubai, United Arab Emirates
Journal homepage: http://saudijournals.com

Original Research Article

Sequential Thermal Regeneration of Activated Carbon Used for Textile Effluent Decolorization

Ismaila Aliyu Oga[1,2]*, Prof. AU Itodo[1], Dr.ME Khan[2,3]

[1]Department of Chemistry, Federal University, Lafia, Nasarawa State, Nigeria
[2]Joseph Sarwuan Tarka University, Makurdi, Benue State, Nigeria
[3]Department of Chemistry, Federal University of Lokoja, Kogi State, Nigeria

DOI: https://doi.org/10.36348/sijcms.2025.v08i06.004 | **Received:** 16.10.2025 | **Accepted:** 08.12.2025 | **Published:** 15.12.2025

***Corresponding author:** Ismaila Aliyu Oga
Department of Chemistry, Federal University, Lafia, Nasarawa State, Nigeria

Abstract

Thermal regeneration of spent commercial granular activated carbon was done sequentially after batch adsorption studies to check the adsorptive capacities of the carbon after four (4) circles of regeneration. Characterization of the adsorbents was carried out instrumentally using FTIR, SEM, and PXRD. Characterization parameters such as burn off 25.06% (CGAC) and 6.498% for (RGAC), bulk density 0.58 g/cm^3 for (CGAC) and 0.68 g/cm^3 for (RGAC), Moisture contents 0.074 and pH 7.0. Attrition 36.24% (CGAC) and 88.92 % (RGAC), Conductivity 1422 µs/cm (CGAC) and 13.85 µs/cm (RGAC). Stock solution of 1000 ppm was prepared; the experimental solution was prepared by using dilution formula to calculate the exact amount of the stock needed to dilute with distilled water to obtain 10,20,30,40, and 50 ppm working standards. 20cm^3 of each working standards of Congo red solution were interacted with 1.0 g of the commercial granular activated carbon in a separate glass flask capped with foil. The maximum adsorption capacity after four circles of thermal regeneration, is approximately 81% overall. Batch adsorption study was carried out to study the effect of experimental variables. (pH, Initial concentration, contact time, adsorbent dosage and temperature). The equilibrium study for the sorption of Congo red was investigated using Langmuir, Freundlich, DubininRadushkevich and Temkin isotherm models. The linearity of the Langmuir isotherm models (R^2 value of 0.9909 for CGAC, 0.9869 for RGAC), Freundlich isotherm model R^2 was CGAC (0.9295), RGAC (0.8794), Temkin isotherm model (R^2 CGAC (0.7837), RGAC (0.8076), and Dubinin-Radushkevich isotherm model RGAC (0.7829), CGAC (0.7322) were obtained from their various plots. Langmuir seems to have the best fit having its R^2 values very close to 1 follow by Freundlich isotherm model. The efficiency in removal of Congo red using the regenerated adsorbent and commercial activated carbon at 95% confidence interval shows that there is no statistically significant difference. This implied that regeneration of adsorbents after use is of economic advantage to curb cost in solving the problem of textile effluents decolorization.

Keywords: Adsorption, Adsorbent, Adsorbate.

INTRODUCTION

One of the biggest environmental issues facing the world today is water pollution brought on by the release of colored effluent from textile dye manufacturing and dyeing mills (Periyasamy 2024). Although dyes give textile fibers, foodstuffs, etc. attractive colors, the bright colors they impart to aquatic habitats cause both aesthetic and ecological issues (Negi (2025).

The majority of dyes are deemed non-oxidazable by standard physical and biological treatment because to their huge sizes and intricate molecular structures (Ayub *et al.*, 2025). Therefore, one of the essential steps in wastewater treatment is their decolorization. Physio-chemical techniques such as adsorption (Tripathi *et al.*, 2023), electrochemical coagulation, and photocatalytic decolorization (Rakhmania *et al.*, 2022) are more common these days. Several techniques have been developed to remove different types of dyes from wastewater in a preferential manner (Tripathi *et al.*, 2023). Adsorption is one of these techniques that is becoming more and more popular due to its simplicity and adaptability. According to Lu *et al.* (2022), it is a practical and straightforward method that enables kinetic and equilibrium measurements without the need for extremely complex equipment.

Because of its unique pore structure and superficial surface-activated activity, activated carbon has been employed for decades in liquid decolorization and refining (Chew *et al.*, 2023). In order to eliminate exhausted carbon, the batch-operated powder activated carbon (PAC) decouring process must be filtered. The use of 10–20 g/L of liquid in the PAC decolorization process raises production costs. Continuous and automated decolorization processes have made use of granular activated carbon (GAC) (Wang *et al.*, 2024). GAC has the advantage of being able to regenerate, which reduces the amount of solid residue, thus enabling continuous operation (Chen *et al.*, 2025). Regenerating and reusing the exhausted GAC is essential, as is the expansion of GAC production and its extensive application in numerous industries (Cansado *et al.*, 2023). In addition to reducing secondary pollution and conserving natural resources, it can also generate significant financial gains (Ahmad *et al*., 2023). Thermal volatilization is the most widely used regeneration approach, whereby adsorbed materials are desorbed through oxidation and volatilization at high temperatures (Wang *et al.*, 2025). The carbon loss (10–15%) from oxidation and attrition, as well as the energy expense of heating the carbon to about 800-9000c, are characteristics of this thermal regeneration approach. Chemical regeneration is an alternate method that involves applying chemical reagents to the depleted carbon (Zhang *et al.*, 2023). In order to restore the activated carbon's adsorption capacity, the adsorbate is typically dissolved using acid and alkali solutions. The current study examined the effects of GAC dosage, duration, and temperature on adsorption effectiveness while using GAC to adsorb pigments and contaminants from CAF liquid (Wasilewska *et al*., 2024).

MATERIALS AND METHOD

Granular Commercial Activated carbon was used in all the experiments, as virgin and regenerated. GAC was used in the decolonization of dye (Congo red). The characterization of the virgin and the regenerated GAC was analyzed. All the chemical used was of analytical reagents (AR) grade and all reagents was prepared freshly with distilled water.

Preparation of Stock and Standard Solution

The stock solution of Congo Red was prepared by adding 1g of the dye to 1000 ml of distilled water by continuous stirring with a glass rod for uniformity.

Batch Experiments

Batch Equilibrium Experiments: A stock solution of 1000ppm was prepared (Munene Mwaniki 2022) for Congo red. The experimental solution was prepared by diluting stock with distilled water to obtain 10,20,30,40, and 50 ppm working standards. 20 cm3 of each working standards of Congo red solution were interacted with 1.0 g of the granular commercial activated carbon in a separate glass flask capped with foil. The flasks were shaken using a thermostatic shaker at 120 rpm and constant temperature of 30 oC. It was assumed that the applied shaking speed allows all the surface area to come in contact with the Congo red over the course of the experiments. After shaking for the desired time (1h), the samples were filtered, using Wattman filter paper and absorbance reading of the Congo red sample was taken at a pre-determined wavelength of 499 nm. The effects of various parameters on the rate of adsorption process were observed by varying contact time, adsorbent dose, adsorbate concentration, temperature, and pH of the solution. The amount of the Congo red adsorbed per unit mass of the granular commercial activated carbon (gL-1) was calculated using the mass balance equation given as:

$$\boldsymbol{qe} = (\boldsymbol{CO}-\boldsymbol{Ce})\boldsymbol{WV}$$

Where: C0 and Ce are initial and equilibrium dye concentrations in mgL-1, respectively, V = Volume of the solution in litres and W=weight of the activated carbon in (g). qe = theoretical maximum adsorption capacity of the activated carbons (mgg-1) (Etsuyankpa et al., 2025; Mathew et al., 2025; Musa et al., 2025)

Thermal Regeneration of Spent Activated carbon

Thermal regeneration was based on the approach of Bunker *et al* (2023). Spent sample of commercial granular activated carbon after batch adsorption experiment was placed in a furnace at 600^{o}C for 5 min. The heated sample was removed and poured into iced water bath and excess water was drained and allowed to stand at room temperature. This procedure was repeated at 800 ^{o}C for 5minutes.

The above procedure was repeated in four (4) cycles. The regenerated activated carbon was washed first with 0.1M HNO3 (Chen *et al.*, 2022) to remove surface ash, and rinsed thoroughly with warm water and finally with distilled water to remove residual chemicals (Habte *et al.*, 2025), and until a pH of 6 was attained (Xia *et al*., 2024). The regenerated granular activated carbon was then oven dried at 105^{0}C and stored for re-use.

Adsorption isotherms

The equilibrium data generated were fitted into the Langmuir, Freundlich, Temkin, and Rudishkevich – Dubinin isotherm models. Best fit models' prediction was based on the correlation of applicability (R2) and the statistical sum of error analysis (Musa et al., 2024; Abdulkadir et al., 2025).

RESULT AND DISCUSSION

Results for Physicochemical Prarameter Adsorbents before and after Regenerated.

Results of the physicochemical parameters of adsorbent was reported as mean value and presented in table 1.

Characterization of Virgin, And Regenerated Activated Carbon.

The adsorbents was characterized as classical where parameters such as pH, bulk density, Attrition,

Burn off, and Conductivity. Also instrumental characterization such as Fourier transforms infrared (FT-IR), Scanning Electron Microscope (SEM), X-Ray Powder Diffraction Analysis (XRD)was characterized.

Classical Characterisation

pH

The standard test method for determination of pH was done using 1.0 g of granular activated carbon (CGAC) Was weigh and transfer into a beaker. 100 ml of distilled water was measured and added and stirred for one hour. The samples was allowed to stabilized before the pH was measured using a pH meter (Nascimento *et al.*, 2025).

Bulk density

The procedure described by (Banerjee, and Chattopadhyay, 2025).). The specific density bottle was weigh and the volume of water which can fill it up to the brim, was measured. The bottle was filled with the adsorbents and weigh.

$$\boldsymbol{Bulkdensity} = \frac{W_2 - W_1}{V} \text{g cm}^{-1}$$

whereW_1 = weight of empty bottle, W_2 = weight of empty bottle and adsorbents, W_2-W_1 = weight of adsorbents, V mL = Volume of the adsorbents or Volume of water needed to fill the bottle.

Burn off

Percentage burn off which is the percentage weight decrease during activation, referred to the weight of the original carbonized product. The % burn off of the carbonized samples during activation was determined by measuring the weight of the samples before and after activation by following formula,

$$\textbf{Burn off} = \frac{W_c - W_a}{W_c} \textbf{X 100}$$

Where,

Wc = Weight of the samples before activation (i.e. weight of the carbonized product)

Wa = Weight of the samples after activation (i.e. weight of the activated carbon).

$$\textbf{V. \%Attrition} = \frac{Initialweight(g) - Finalweight\ (g)}{Initialweight\ (g)} \textbf{ X 100}$$

Table 1

S/N	Parameters	Adsorbent CGAC	RGAC
1.	pH	7±0.05	6±0.02
2.	Bulk density g/cm^3	0.58±0.23	0.67±0.02
3	Moisture contents%	0.98±0.04	1.04±0.08
4	Burn off %	25.06±0.20	6.49±0.23
5	Attrition %	36.24±043	88.92±0.03

Instrumental Characterisation

Fourier transform infrared (FT-IR)

The Fourier transform infrared (FT-IR), spectroscopic analysis was perform using (Cary 630 by Agilent Technology USA) to study the surface chemistry of the *regenerated activated carbon*. The FT-IR spectra of the absorbents before and after Regeneration was taken.

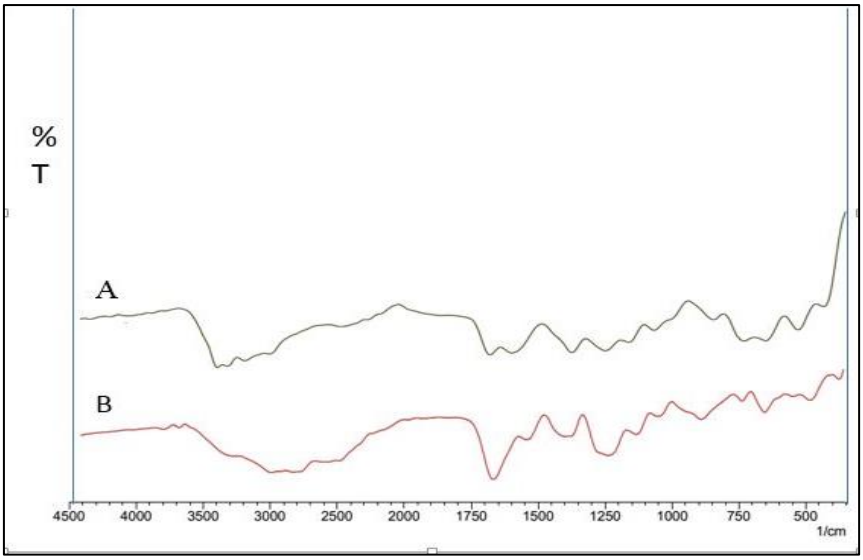

Figure 1

S/No	Group frequencies (Cm-1)	Observed frequencies CGAC	RGAC	Functional group
1.	1000-100	410.29,420.31, 432.24,454.36;	406.40,420.62; 445.03	C-H
2.	1500-1000	108969;	1033.16,1055.00;	C-O Stretch; CH_3 Symmetric deformation; N-O
3.	1500-1250	1577.10; 1684.3;	1560.06,1654.60;	N-N bend; C≡C Stretch; C=C Stretch
4.	2500-1750	2209.18,2072.79;	2066.27,2190.96;	N=N=N, Anti-Symmetric; Stretch. C≡N; -PH; C≡N
5.	3500-2500	3261.76;		O-H Broad; O-H Stretch; -NH Stretch; ≡CH-H Stretch

Figure 2

Scanning electron microscope (SEM)

Scanning electron microscopy was used to study the morphology of the regenerated activated carbon. The SEM images of the absorbents before and after regeneration were obtained. (The SEM model used is Phenomworld Eindhoven the Netherland). The Scanning Electron Microscope (SEM) image of commercial and thermally regenerated activated carbon after four cycle (4) of regenetion at selected magnifications was observed. The micrograph displayed the surface structure or morphology of the adsorbent are shown below.

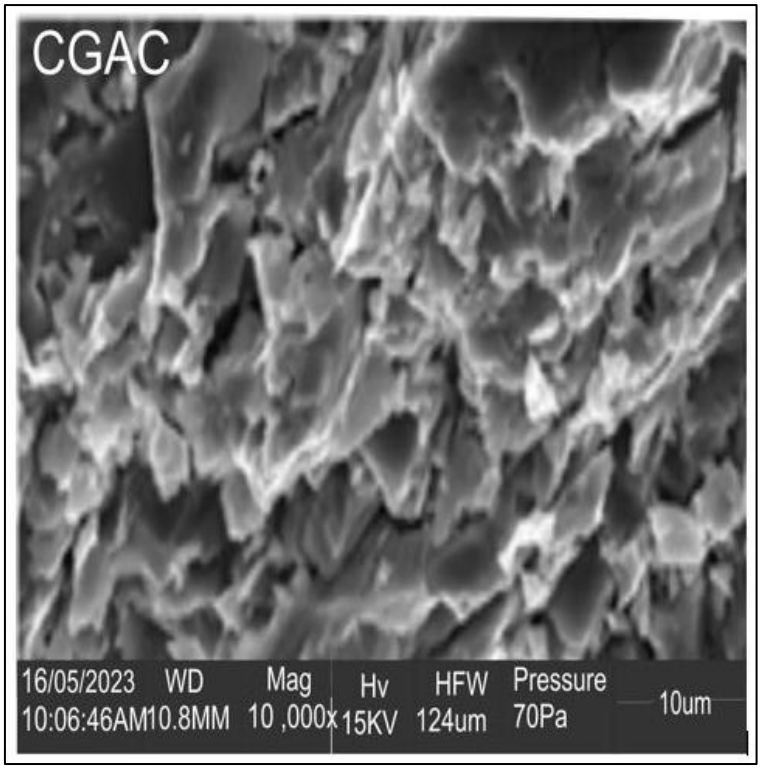

Figure 3

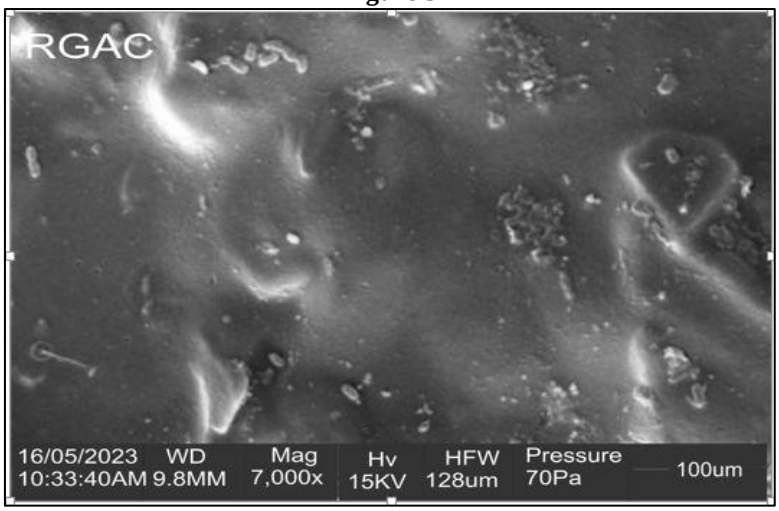

Figure 4

X-Ray Difractometer

X-ray diffraction (XRD) is a material characterization technique that was used for analyzing the lattice structure of a material. Powder X-ray diffraction (PXRD) patterns were recorded on a BRUKER –AXS D8 Advanced X-ray Diffractometer (Rigaku miniflex 600 by Rigaku cooperation Japan) with Cu–Kα radiation machine at the Department of Chemistry, Ahmadu Bello University Zaria. The X- ray diffraction data were recorded by using Cu Kα radiation (1.5406 A^0). The relative intensity data were collected over a 2θ range of 10–40°C.

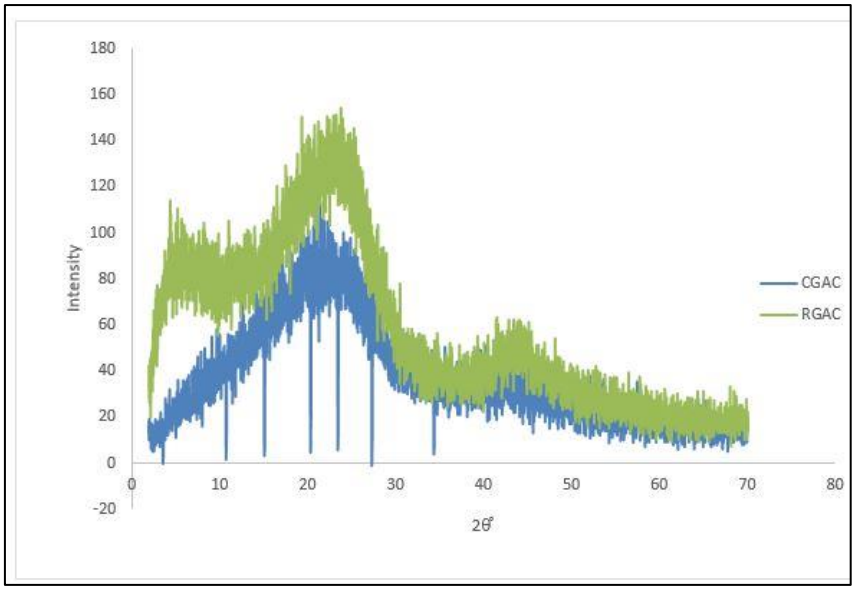

Figure 5

Adsorption Parameters

Parametric factors such as effect of initial concentration, pH, time, adsorbent dose and temperature were varied in order to compare the working parameters.

Effect of initial concentration

Figure 6,7,8,9 and 10 represents the effect of initial concentration on adsorption of Congo red over virgin granular carbon and thermally regenerated carbon after four cycle of regeneration varying from Time 20, 40, 60, 80 and 100min, while other parameters were kept constant (30 ± 2 ºC, pH of 6.0, 250 rpm)

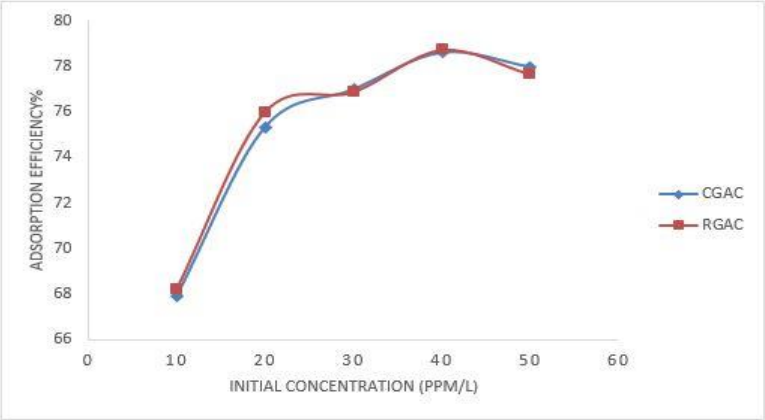

Fig 6: Effect of Initial Sorbate Concentration on Adsorption of Congo red on CGAC and RGAC at 30 ± 2 ºC, Time 20 min, pH of 6.0, 250 rpm

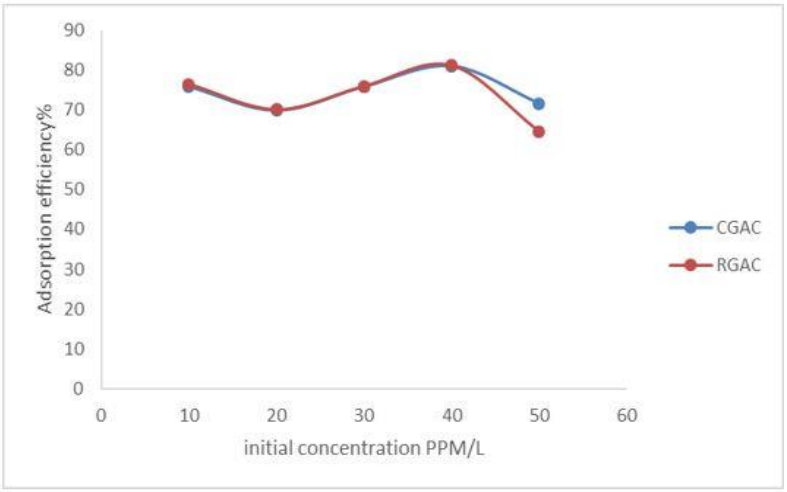

Fig 7: Effect of Initial Sorbate Concentration on Adsorption of Congo red on CGAC and RGAC at 30 ± 2 °C, Time 40 min, pH of 6.0, 250 rp

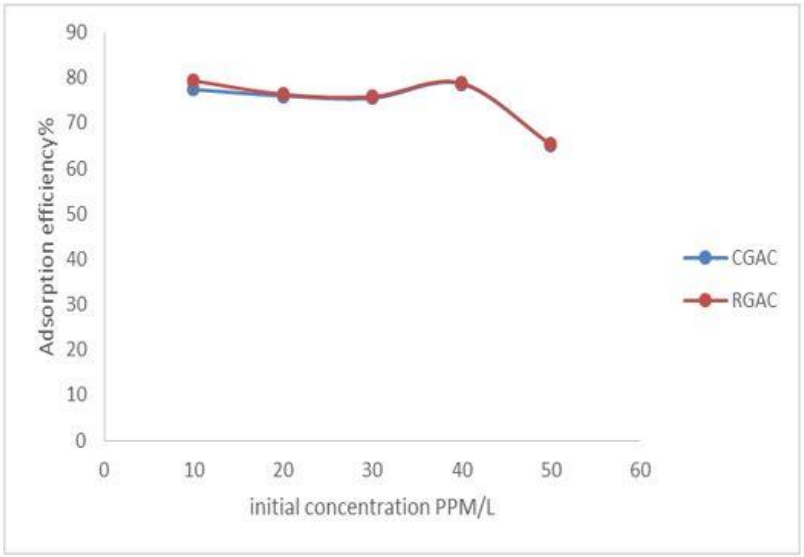

Fig 8: Effect of Initial Sorbate Concentration on Adsorption of Congo red on VCAC and RGAC at 30 ± 2 °C, Time 60min, pH of 6.0, 250 rpm.

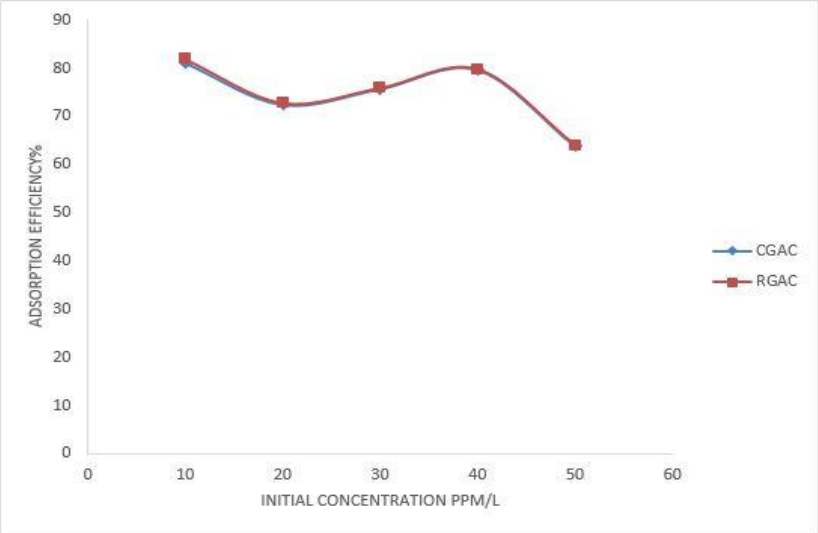

Fig 9: Effect of Initial Sorbate Concentration on Adsorption of Congo red on CGAC and RGAC at 30 ± 2 °C, Time 80 min, pH of 6.0, 250 rpm.

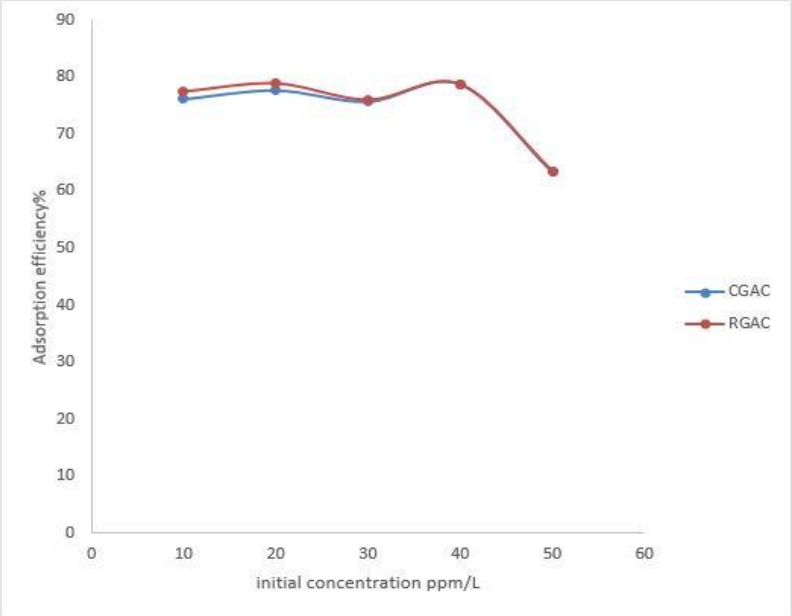

Figure 10: Effect of Initial sorbate concentration of adsorption of Congo red on Commercial granular activated carbon (CGAC) and regenerated granular activated carbon (RGAC). at 30 ± 2°C, Time 100min, pH of 6.6, 250rpm.

Effect of dosage on adsorbent

Figures 11,12,13,14 and 15 shows, the effect of adsorbent dose on the removal efficiency of Congo red on CGAC and RGAC, by varying time and concentration, other parameters kept constant 30 ± 2 °C and pH 6.0,250 rpm

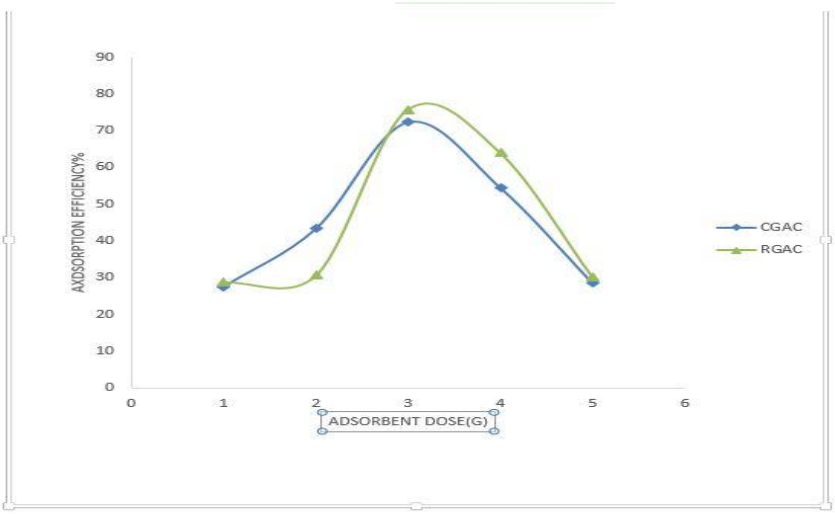

Fig 11: Effect of Adsorbent Dose on Percentage Adsorption of Congo red on CGAC and RGAC at 30 ± 2 °C, 10 ppm/L, Time 20 min and pH of 6.0

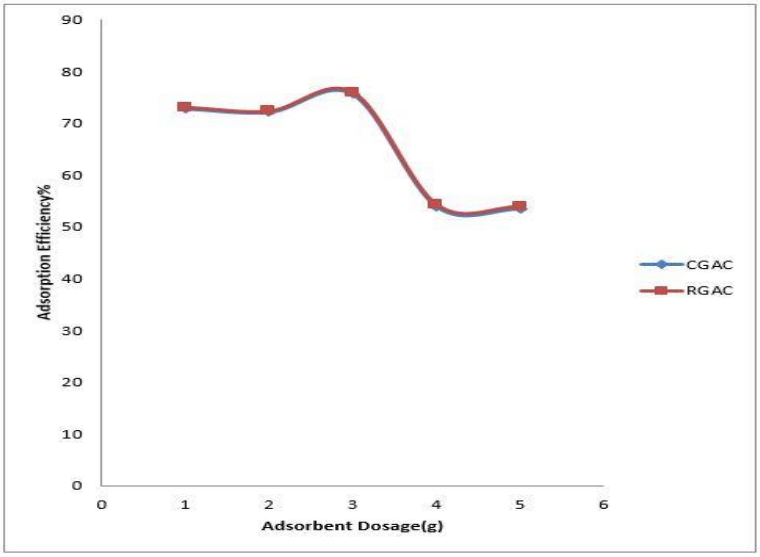

Fig 12: Effect of Adsorbent Dose on Percentage Adsorption of Congo red on CGAC and RGAC at 30 ± 2 °C, 20 ppm/L, time 60 min and pH of 6.0, 250 rpm

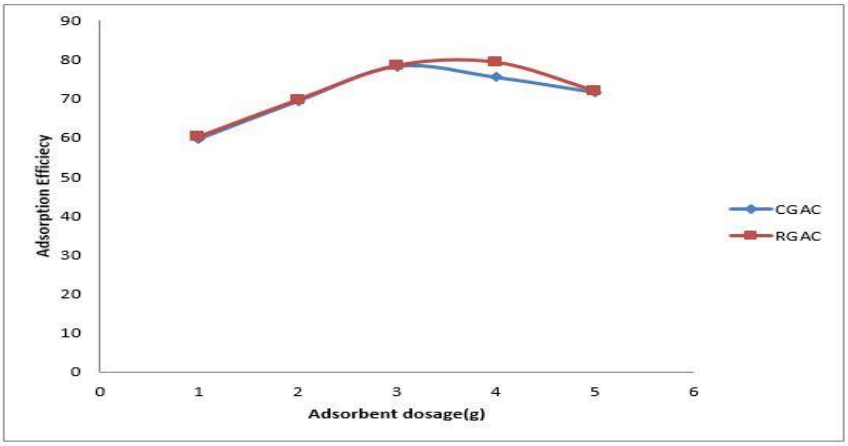

Fig 13: Effect of Adsorbent Dose on Percentage Adsorption of Congo red on CGAC and RGAC at 30 ± 2 °C, 30 ppm, Time 40 min and pH of 6.0, 250 rpm.

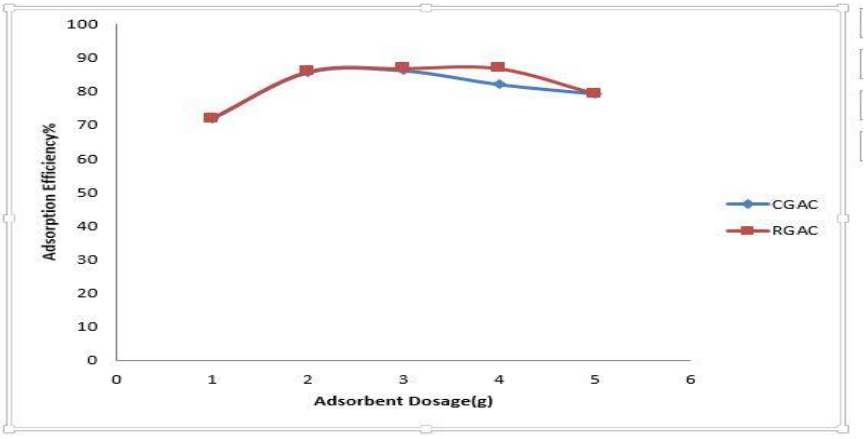

Fig 14: Effect of Adsorbent Dose on Percentage Adsorption of Congo red on CGAC and RGAC at 30 ± 2 °C, 40 ppm/L, Time 80 min and pH of 6.0, 250 rpm.

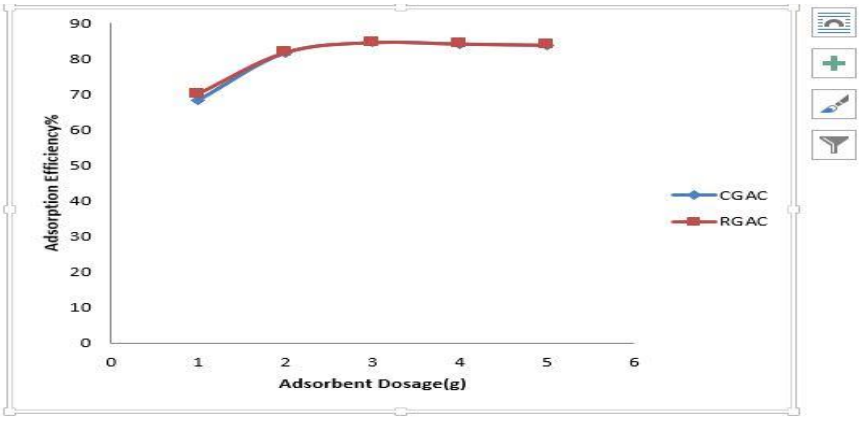

Fig 15: Effect of Adsorbent Dose on Percentage Adsorption of Congo red on CGAC and RGAC at 30 ± 2 °C, 50 ppm/L, Time 100 min and pH of 6.0, 250 rpm

Effect of contact time on adsorption

Figures 16, 17, 18,19 and 20 shows the effect of contact time on the percentage adsorption of Congo red on CGAC and RGAC after four cycles of thermal regeneration for varied concentrations 10, 20, 30, 40 and 50 ppm while other parameters were kept at pH of 6.0, 250 rpm and 1.0 g adsorbent dose.

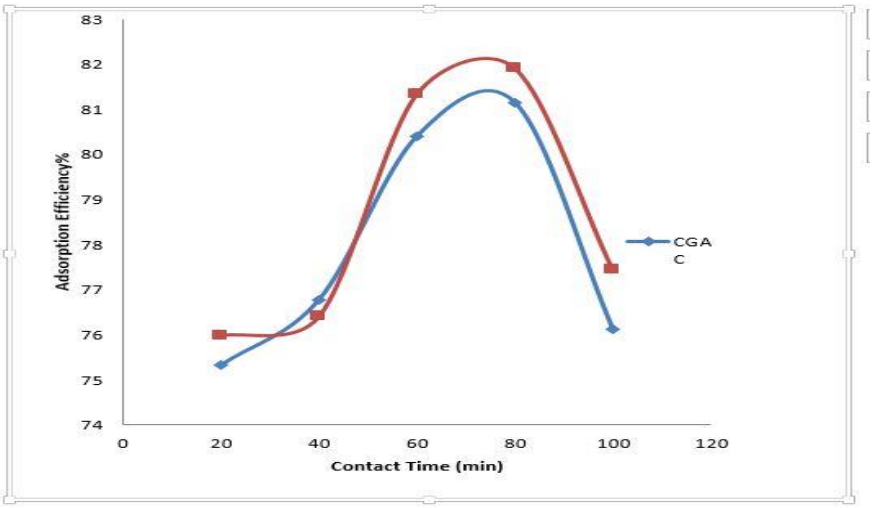

Fig 16: Effect of Contact Time on Percentage Adsorption of Congo red on CGAC and RGAC at 30 ± 2°C, 10 ppm/L 250 rpm and 1.0 g Adsorbent Dose.

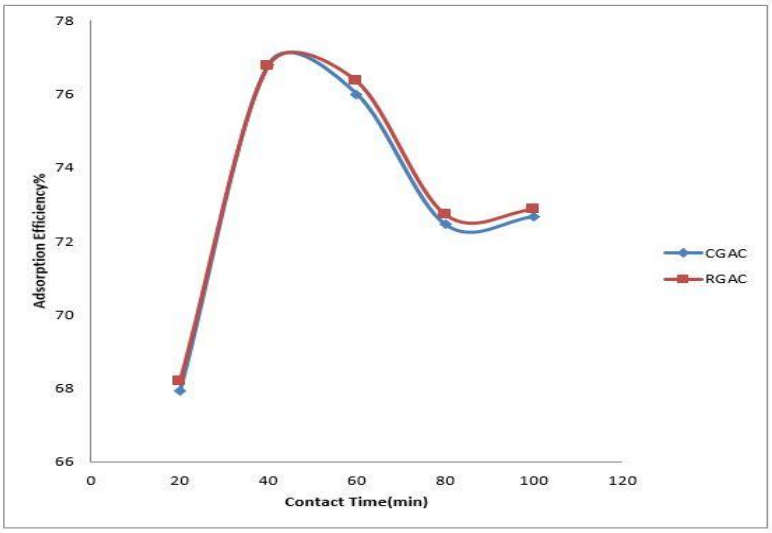

Fig 17: Effect of Contact Time on Percentage Adsorption of Congo red on CGAC and RGAC t 30 ± 2 °C, 20 ppm/L, 250 rpm and 1.0 g Adsorbent Dose

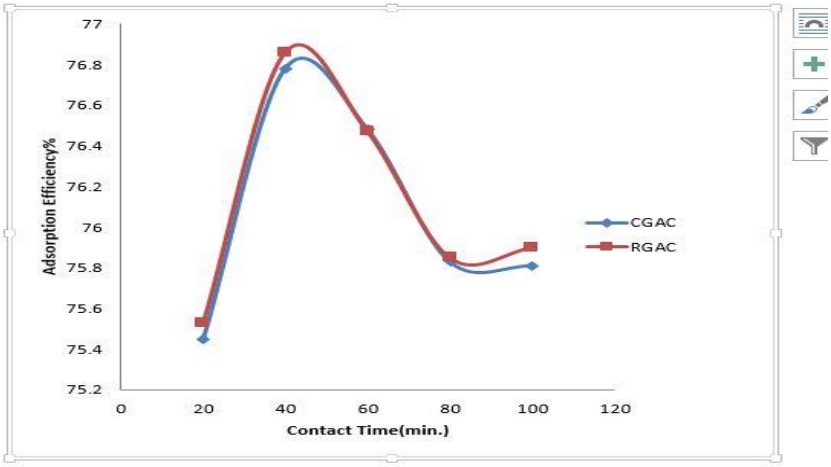

Fig 18: Effect of Contact Time on Percentage Adsorption of Congo red on CGAC and RGAC at 30 ± 2 °C, 30 ppm/L, 250 rpm and 1.0 g Adsorbent Dose, 250 rpm

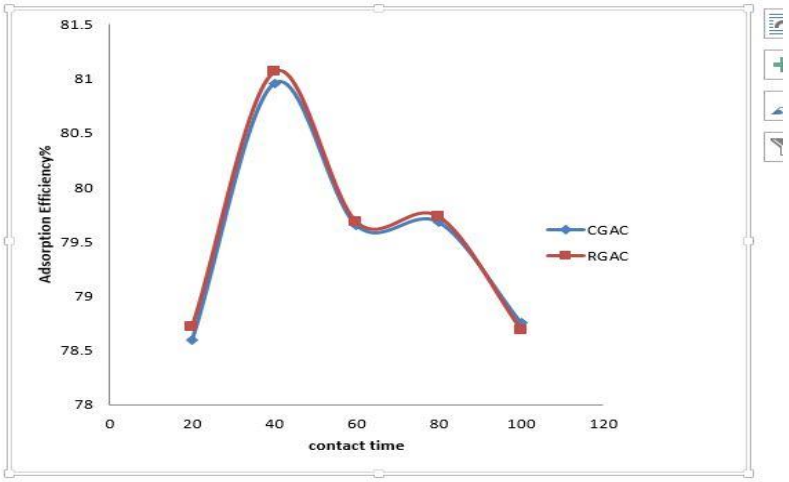

Fig 19: Effect of Contact Time on Percentage Adsorption of Congo red on VCAC and RGAC at 30 ± 2°C, 40 ppm /L 250 rpm and 1.0 g Adsorbent Dose

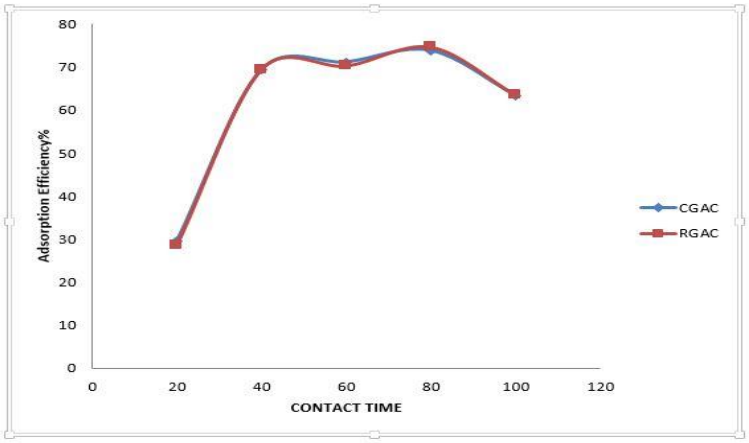

Fig 20: Effect of Contact Time on Percentage Adsorption of Congo red on CGAC and RGCAC at 30 ± 2 °C, 50 ppm/L, 250 rpm and 1.0 g Adsorbent Dose, 250 rpm

Effect of temperature on adsorption

Figure 21, 22, 23, 24 and 25 shows the effect of temperature on the percentage of adsorption of Congo red on CGAC and RGAC by varying concentration while other parameters are kept at pH of 6.0, 250 rpm and 1.0 g adsorbent dose.

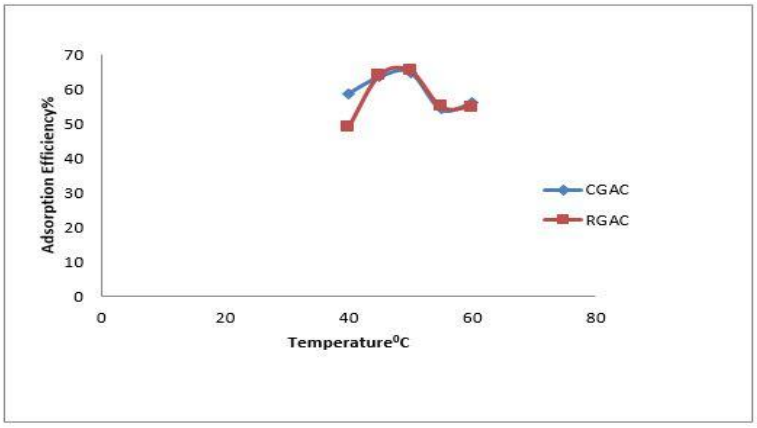

Fig 21: Effect of temperature on Percentage Adsorption of Congo red on CGAC and RGCAC at 10 ppm/L, 250 rpm and 1.0 g Adsorbent Dose.

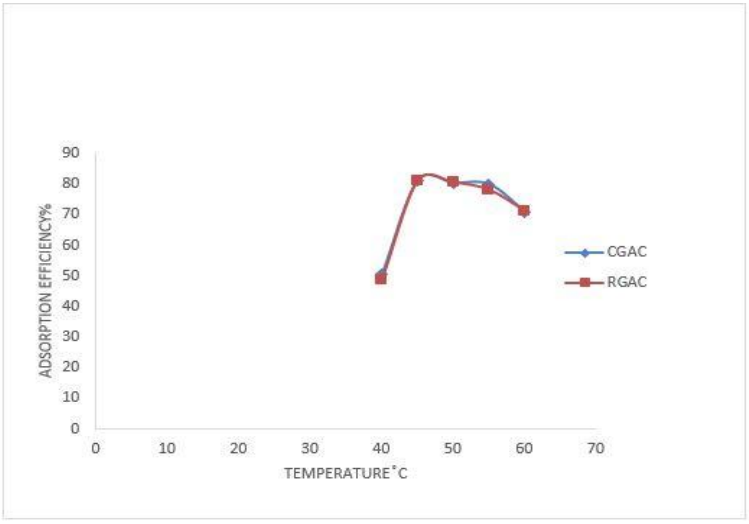

Fig 22: Effect of temperature on Percentage Adsorption of Congo red on CGAC and RGAC, 20 ppm/L, at 250 rpm and 1.0 g Adsorbent Dose

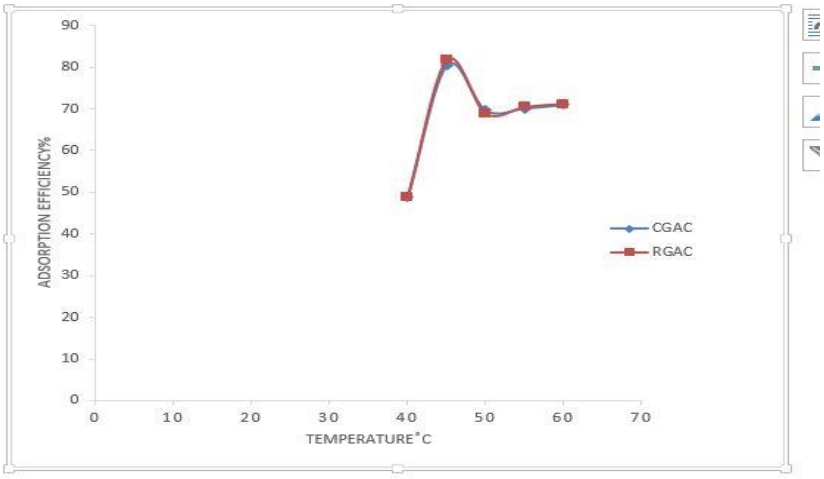

Fig 23: Effect of temperature on Percentage Adsorption of Congo red on CGAC and RGCAC at 30 ppm/L, 250 rpm and 1.0 g Adsorbent Dose

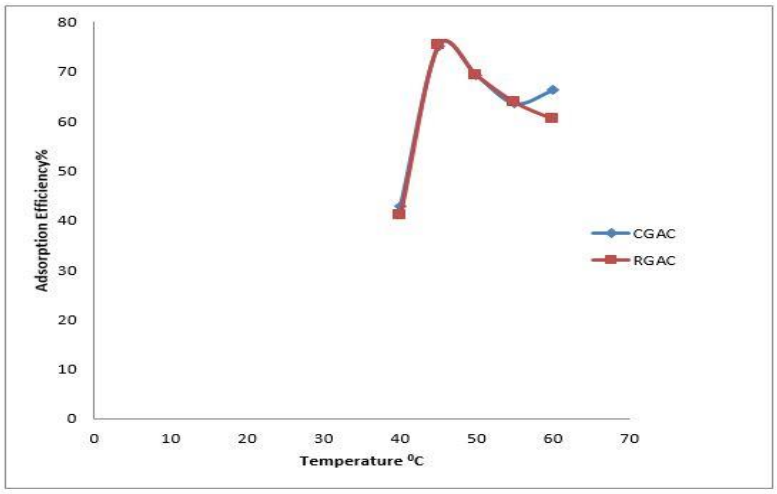

Fig 24: Effect of temperature on Percentage Adsorption of Congo red on CGAC and GRAC at 40 ppm/L, 250 rpm and 1.0 g Adsorbent Dose

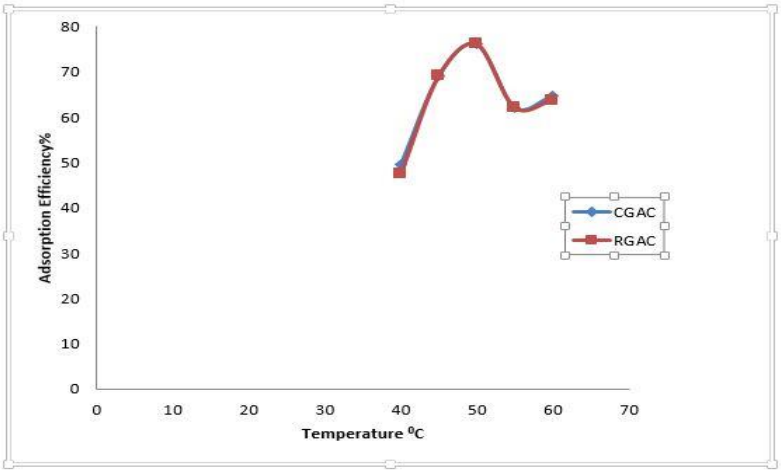

Fig 25: Effect of temperature on Percentage Adsorption of Congo red on CGAC and RGAC at 50 ppm/L, 250 rpm and 1.0 g Adsorbent Dose

Effect of pH on adsorption

Figures 26,27,28,29 and 30 shows effect of pH on percentage adsorption of Congo red on CGAC and RGAC after the fourth regeneration by varying the concentration at 10ppm ,20ppm,30ppm,40 ppm and 50 ppm, other parameters kept at 30 ± 2 °C, 250 rpm and 1.0 g adsorbent dose, 250 rpm.

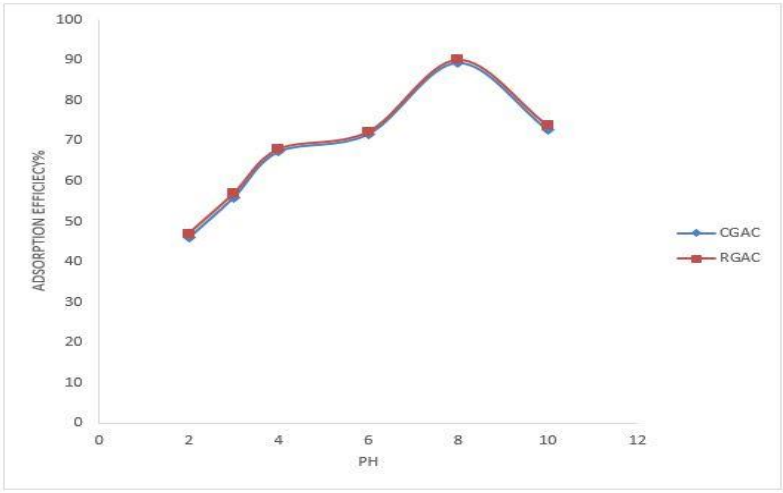

Fig 26: Effect of pH on Percentage of Adsorption Congo red on CGAC and RGAC at 30 ± 2 °C, 10ppm/L, 250 rpm and 1.0 g Adsorbent Dose.

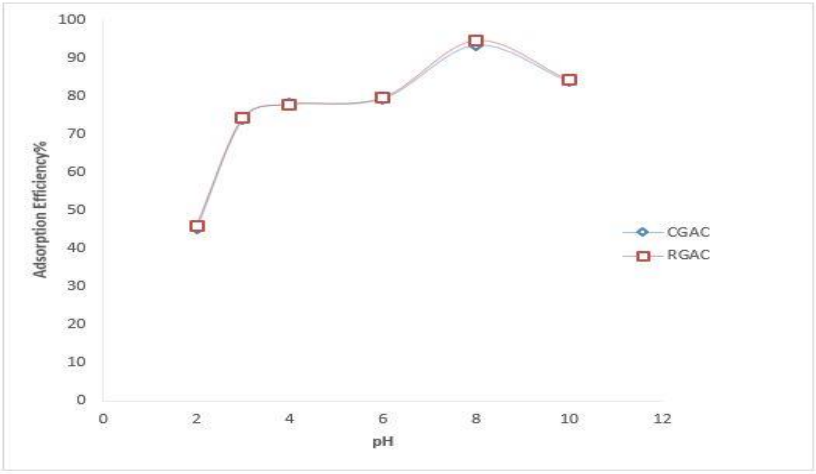

Fig 27: Effect of pH on Percentage of Adsorption Congo red on CGAC and RGAC at 30 ± 2 °C, 20 ppm/L, 250 rpm and 1.0 g Adsorbent Dose

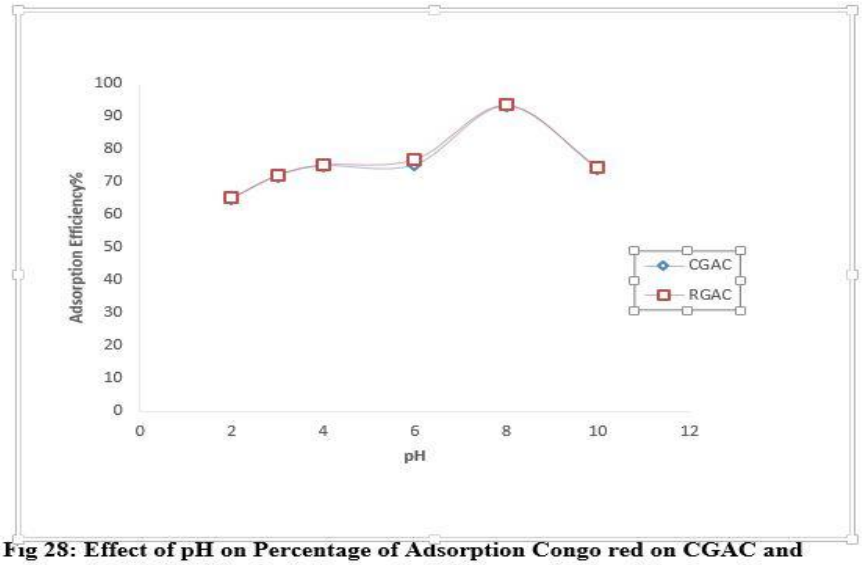

Fig 28: Effect of pH on Percentage of Adsorption Congo red on CGAC and RGAC at 30 ± 2 °C, 30 ppm/L, 250 rpm and 1.0 g Adsorbent Dose

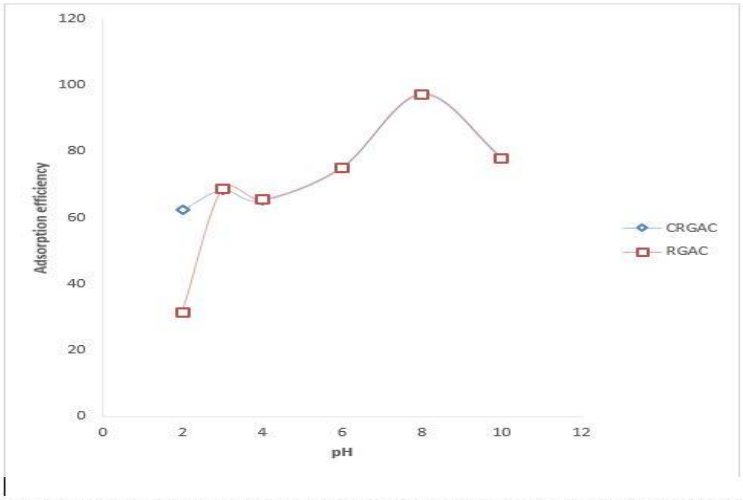

Fig 29: Effect of pH on Percentage of Adsorption Congo red on CGAC and RGAC at 30 ± 2 °C, 40 ppm/L, 250 rpm and 1.0 g Adsorbent Dose

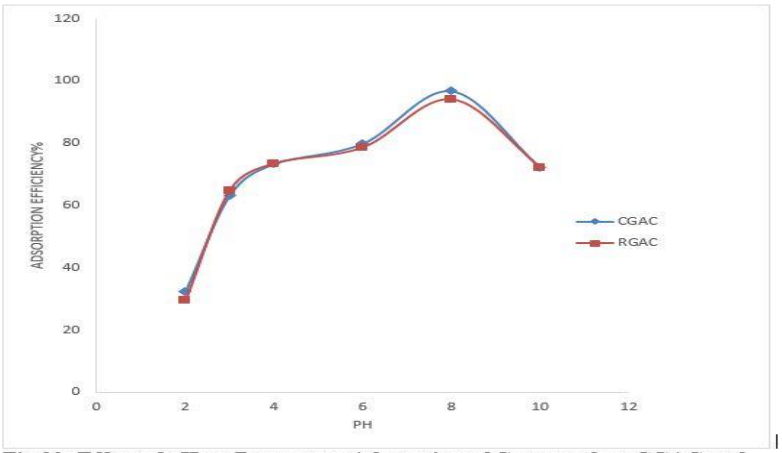

Fig 30: Effect of pH on Percentage Adsorption of Congo red on CGAC and RGAC at 30 ± 2°C, 50PPM/L, 250rpm and 1.0g Adsorbent Dose

Adsorption Isotherms

Four adsorption isotherm equations were adopted for the modeling of the adsorption experimental data.

Langmuir isotherm

Figure 31 and 32 shows Langmuir isotherm plot of Congo red adsorption on CGAC and RGAC adsorbents. Which is used to describe the equilibrium between the adsorbents and the adsorbate system.

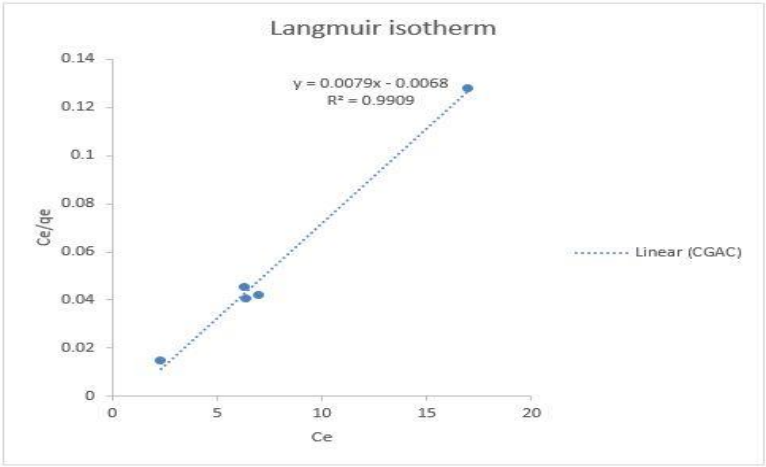

Figure 31: Langmuir isotherm plot of Congo red adsorption for the commercial granular activated carbon (CGAC) adsorbents.

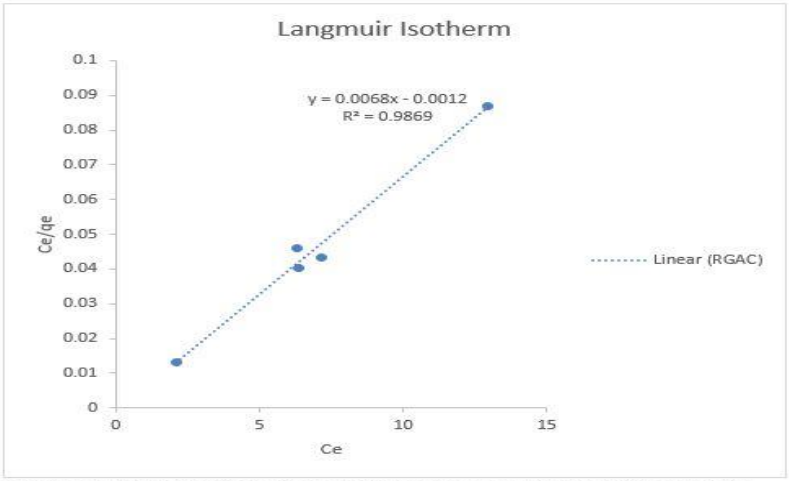

Figure 32: Langmuir isotherm plot of Congo red adsorption for the regenerated granular activated carbon (RGAC) adsorbents

Freundlich isotherm

Figure 33 and 34 shows Freundlich isotherm plot of Congo red adsorption on CGAC and CGACadsorbents. This was used to predicts the variation in the dye adsorbed by the solid at constant temperature and pressure.

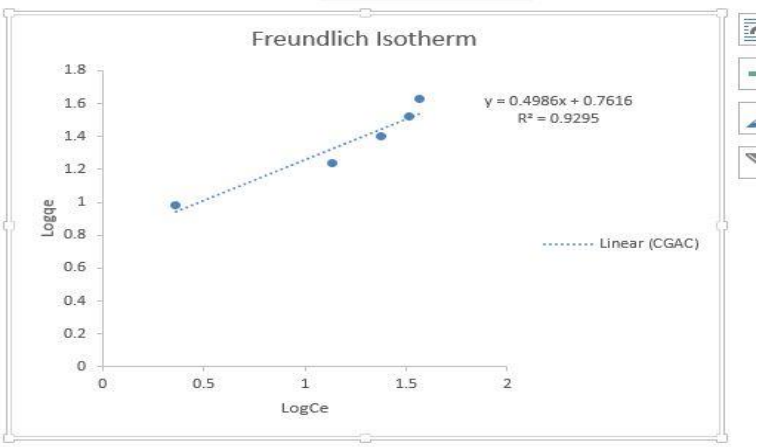

Fig 33: Freundlich Isotherm Plot of Congo red Adsorption on CGAC Adsorbent

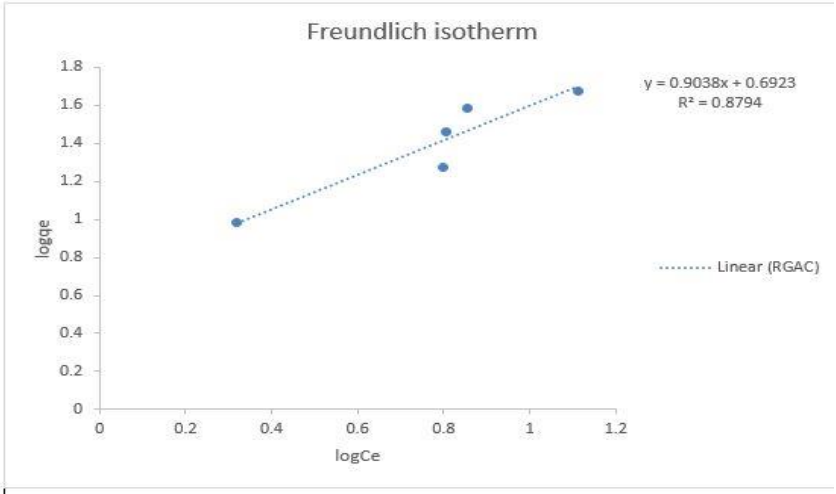

Fig 34: Freundlich Isotherm Plot of Congo red Adsorption on regenerated (RGAC) Adsorbent

Temkin isotherm

Figure 35 shows Temkin isotherm plot of Congo red adsorption over CGAC adsorbent. This was used to predicts multilayer adsorption between adsorbate and adsorbent.

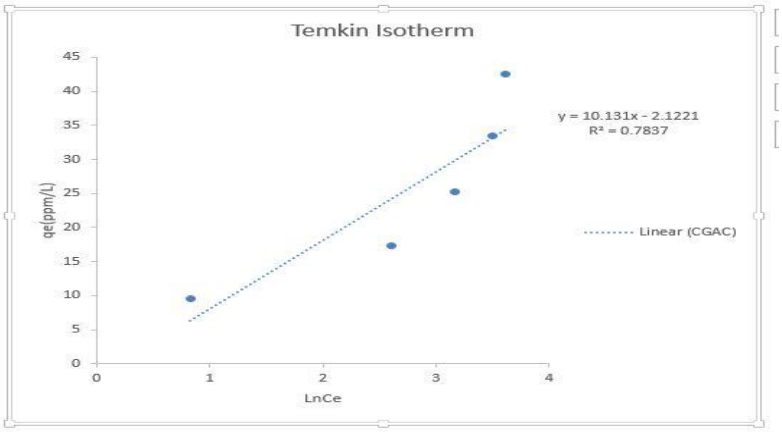

Fig 35: Temkin Isotherm Plot of Congo red Adsorption on CGAC Adsorbent

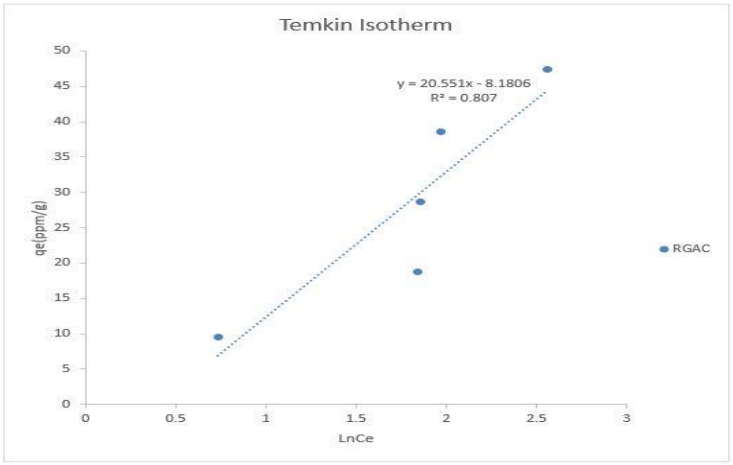

Fig 36: Temkin Isotherm Plot of Congo red Adsorption on regenerated (RGAC) Adsorbent

Dubinin–Radushkevich isotherm

Figure 37 represent Dubinin–Radushkevich plot of Congo red adsorption over CGAC adsorbent. This was meant to quantitatively describe the adsorption of gases and vapors by microporous sorbents.

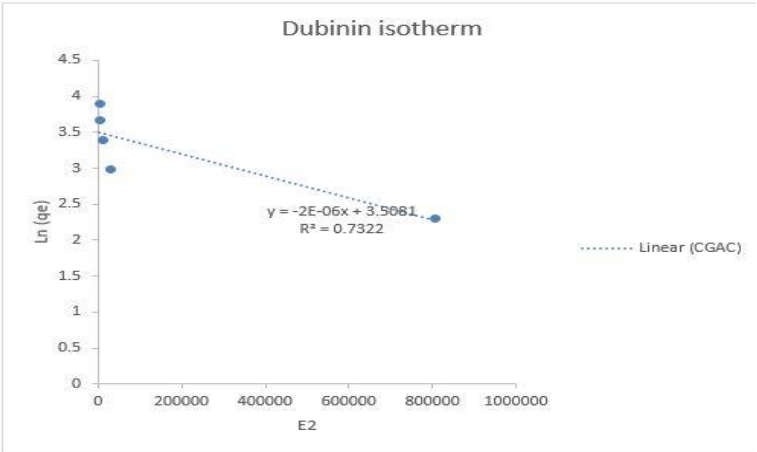

Fig 37:Dubinin–Radushkevich Plot of Congo red Adsorption on CGAC and RGAC Adsorbents

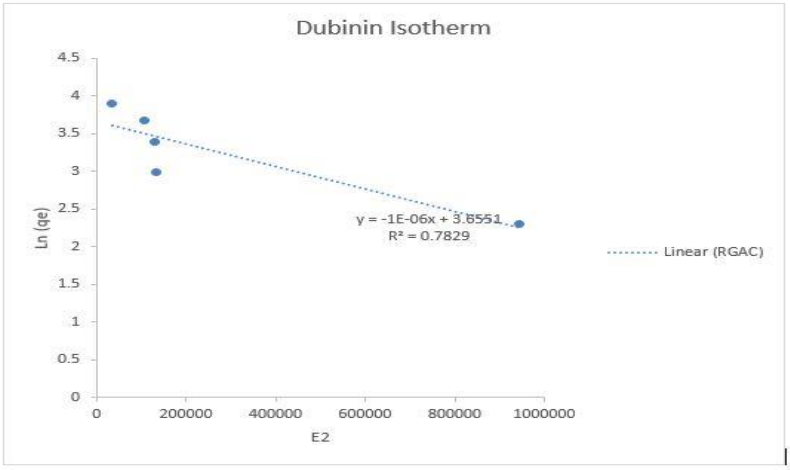

Fig 38: Dubinin–Radushkevich Plot of Congo red Adsorption on RGAC Adsorbents

Isotherms	Constant/Units	CGAC	RGAC
Langmuir	qe	165.31	164.27
	K_L	1.165	5.667
	R^2	0.9909	0.9869
Freundlich	$K_{F\ (mg/g)}$	5.7756	4.9238
	I/n	0.4986	0.9038
	R^2	0.9295	0.8794
Temkin	$b_{T\ (KJ/mol)}$	10.131	20.551
	K_T	1.2330	2.5007
	R^2	0.7837	0.8076
Dubinin-Raduskevch	q_m	1.516	1.000
	E (KJ/mol)	0.3775	0.3699
	R^2	0.7322	0.7829

Statistical test for significance

Experiment	Adsorbent	P-Values	Difference (P≥ 0.05)
Effect of initial concentration	CGAC and RAC	1.000	Not significant
Effect of pH	CGAC and RAC	1.000	Not Significant
Effect of Adsorbent Dosage	CGAC and RAC	1.000	Not Significant
Effect of Contact Time	CGAC and RAC	1.005	Not Significant
Effect of Temperature	CGAC and RAC	1.085	Not Significant

CONCLUSION

The commercial activated carbon (absorbent) has been successfully regenerated sequentially in four circle after batch adsorption studies. After the sequential regeneration taken, there was a significant high adsorption capacity. The commercial and the generated adsorbents were characterized.

The congo red (dye) is adsorbed on CAC and regenerated carbon in batch mode. The effects of various operating conditions, like, pH, initial dye concentration, temperature, etc., are investigated. More than 85% adsorption is observed to take place within 40 to 60 min for the initial concentration of 10 ppm. It is found that adsorption is ~90% for the initial dye concentrations of 10–50 ppm at pH 6.0. The percentage adsorption decreases to 87, 63 and 25% for the initial dye concentrations of 40 and 50 ppm/L, respectively, at the end of the experiment when the pH is 10.

Investigated isotherms show that all adsorption fitness to the models follows similar trends with close R^2 values. The best fit coefficient of regression value for the adsorbents CGAC follow the order; Langmuir> Freundlich > Temkin > Dubinin-Radushkevich.

Among the characterization techniques were PXRD, SEM, Uv-vis and FT-IR spectroscopy. The PXRD reveals the phase crystallinity of the adsorbents and the SEM was used to get the morphology. The FT-IR were used to investigate the particle size distribution and functional group determination respectively.

REFERENCES

- Abdulkadir, A., Musah, M., Lakan, I. I. & Mathew, J. T. (2025). Production of MgO/ZnO Nanocomposite for the Removal of Selected Toxic Metals from Tannery Wastewater. Scholars International Journal of Chemistry and Material Sciences, 8(5): 250-262. https://doi.org/10.36348/sijcms.2025.v08i05.008
- Ahmad, M., Ahmed, Z., Yang, X., & Can, M. (2023). Natural Resources Depletion, Financial Risk, and Human Well-Being: What is the Role of Green Innovation and Economic Globalization? *Social indicators research*, *167*(1-3), 269–288. https://doi.org/10.1007/s11205-023-03106-9
- Ayub, A., Wani, A. K., Chopra, C., Sharma, D. K., Amin, O., Wani, A. W., Singh, A., Manzoor, S., & Singh, R. (2025). Advancing Dye Degradation: Integrating Microbial Metabolism, Photocatalysis, and Nanotechnology for Eco-Friendly Solutions. *Bacteria*, *4*(1), 15. https://doi.org/10.3390/bacteria4010015
- Banerjee, S., & Chattopadhyay, B. (2025). Multi-Stage Methods for Cost Controlled Data Compression Using Principal Component Analysis. *Mathematics*, *13*(13), 2140. https://doi.org/10.3390/math13132140
- Bunker, B., Dvorak, B., & Aly Hassan, A. (2023). Thermal Regeneration of Activated Carbon Used as an Adsorbent for Hydrogen Sulfide (H_2S). *Sustainability*, *15*(8), 6435. https://doi.org/10.3390/su15086435
- Cansado, I. P. d. P., Mourão, P. A. M., & Castanheiro, J. E. d. S. F. (2023). Performance of Regenerated Activated Carbons on Pesticides Removal from the Aqueous Phase. *Processes*, *11*(8), 2496. https://doi.org/10.3390/pr11082496
- Chen, R., Meng, J., Tan, S., Liang, L., Wang, F., Liu, H., Guo, C., Bao, W., Zhang, G., & Yu, F. (2025). Plasma-Assisted Regeneration of Activated Carbon: Current Status and Prospects. *Inorganics*, *13*(7), 209. https://doi.org/10.3390/inorganics13070209
- Chen, W.-S., Chen, Y.-C., & Lee, C.-H. (2022). Modified Activated Carbon for Copper Ion Removal from Aqueous Solution. *Processes*, *10*(1), 150. https://doi.org/10.3390/pr10010150
- Chew, T. W., H'Ng, P. S., Luqman Chuah Abdullah, B. C. T. G., Chin, K. L., Lee, C. L., Mohd Nor Hafizuddin, B. M. S., & TaungMai, L. (2023). A Review of Bio-Based Activated Carbon Properties Produced from Different Activating Chemicals during Chemicals Activation Process on Biomass and Its Potential for Malaysia. *Materials*, *16*(23), 7365. https://doi.org/10.3390/ma16237365
- Etsuyankpa, B. M., Musa, S. T., Ambo, A. I., Sulaiman, L.A., Mathew, J. T. (2025). Removal of Cu^{2+}, Fe^{3+} and Pb^{2+} from Abbatoir Wastewater Using TiO_2/CdS Nanocomposite: Isotherm and Kinetics Studies. *Scholars International Journal of Chemistry and Material Sciences*, *8*(6): 300-310. https://doi.org/10.36348/sijcms.2025.v08i06.002
- Habte, G.A., Bullo, T.A. & Ahmed, Y. (2025). Statistical optimization characterizations and Eco-friendly synthesis of silica from sugarcane bagasse. *Sci Rep* 15, 8492. https://doi.org/10.1038/s41598-025-89366-6
- Lu, Y., Thomas, S., & Zhang, T. J. (2022). Concurrent AtC Multiscale Modeling of Material Coupled Thermo-Mechanical Behaviors: A Review. *CivilEng*, *3*(4), 1013-1038. https://doi.org/10.3390/civileng3040057
- Mathew, J. T., Inobeme, A., Shaba, E. Y., Musah, M., Azeh, Y., Abubakar, H., Adam, I. B., Muhammad, A. I., Muhammad, H. A., Ismail, H., Umar, M. T., Aliyu, M. S., Yisa, S. P., Ismaila, A. O., Etsuyankpa, M. B., Musa, S. T., Mamman, A. (2025). Adsorptive Removal of Cu^{2+}, Pb^{2+}, and Cr^{6+} from Pharmaceutical Wastewater Using Graphene/Rutile (TiO_2) Nanocomposites. Science World Journal, 20 (3), 1263-1272. https://dx.doi.org/10.4314/swj.v20i3.50
- Munene Mwaniki, J. (2022). Adsorption and Its Applications: Using Zinc Adsorption on Water

Hyacinth to Elaborate the Kinetics and Thermodynamics of Adsorption. IntechOpen. doi: 10.5772/intechopen.104293

- Musa A. V., Musah, M. and Mathew, J. T. (2024). Production and characterization of Zeolite-A nanoparticles for the treatment of pharmaceutical wastewater. Science World Journal Vol. 19(4), 987-993. https://dx.doi.org/10.4314/swj.v19i4.11.
- Musa, S. T., Etsuyankpa, B. M., Adamude, F. A., Muhammad, I. H., & Mathew, J. T. (2025). Production of NiO/CuO Nanocomposite for the Removal of Cr^{6+}, Fe^{3+}, and Pb^{2+} from Pharmaceutical Wastewater. *Sch Int J Chem Mater Sci*, *8*(6): 290-299. https://doi.org/10.36348/sijcms.2025.v08i06.001
- Nascimento, T. R. d. L., Guérin, A. L., Rodrigues, M. S., da Silva, C. F., Maciel, B. M., Alhotan, A., Alhijji, S., Velo, M. M. A. C., & Castellano, L. R. C. (2025). 3D Nanofibrous Scaffolds for Encapsulation-Controlled Vancomycin Delivery: Antibacterial Performance and Cytocompatibility. *Polymers*, *17*(23), 3116. https://doi.org/10.3390/polym17233116
- Negi, A. (2025). Environmental Impact of Textile Materials: Challenges in Fiber–Dye Chemistry and Implication of Microbial Biodegradation. *Polymers*, *17*(7), 871. https://doi.org/10.3390/polym17070871
- Periyasamy, A. P. (2024). Recent Advances in the Remediation of Textile-Dye-Containing Wastewater: Prioritizing Human Health and Sustainable Wastewater Treatment. *Sustainability*, *16*(2), 495. https://doi.org/10.3390/su16020495
- Rakhmania, Kamyab, H., Yuzir, M. A., Abdullah, N., Quan, L. M., Riyadi, F. A., & Marzouki, R. (2022). Recent Applications of the Electrocoagulation Process on Agro-Based Industrial Wastewater: A Review. *Sustainability*, *14*(4), 1985. https://doi.org/10.3390/su14041985
- Tripathi, M., Singh, S., Pathak, S., Kasaudhan, J., Mishra, A., Bala, S., Garg, D., Singh, R., Singh, P., Singh, P. K., Shukla, A. K., & Pathak, N. (2023). Recent Strategies for the Remediation of Textile Dyes from Wastewater: A Systematic Review. *Toxics*, *11*(11), 940. https://doi.org/10.3390/toxics11110940
- Wang, Y., Chen, W., Chen, Y., Zhang, S., & Deng, B. (2025). Volatilization and Retention of Metallic and Non-Metallic Elements During Thermal Treatment of Fly Ash. *Materials (Basel, Switzerland)*, *18*(6), 1319. https://doi.org/10.3390/ma18061319
- Wang, Y., Yu, S., & Cai, W. (2024). Study on an Integrated Water Treatment System by Simultaneously Coupling Granular Activated Carbon (GAC) and Powdered Carbon with Ultrafiltration. *Separations*, *11*(11), 312. https://doi.org/10.3390/separations11110312
- Wasilewska, M., Derylo-Marczewska, A., & Marczewski, A. W. (2024). Comprehensive Studies of Adsorption Equilibrium and Kinetics for Selected Aromatic Organic Compounds on Activated Carbon. *Molecules (Basel, Switzerland)*, *29*(9), 2038. https://doi.org/10.3390/molecules29092038
- Xia, Y., Feng, J., Zhang, H., Xiong, D., Kong, L., Seviour, R., & Kong, Y. (2024). Effects of soil pH on the growth, soil nutrient composition, and rhizosphere microbiome of *Ageratina adenophora*. *PeerJ*, *12*, e17231. https://doi.org/10.7717/peerj.17231
- Zhang, T., Yang, Y., Li, X., Zhou, Z., & Wei, B. (2023). Ultrasonic–Thermal Regeneration of Spent Powdered Activated Carbon. *Sustainability*, *15*(11), 9060. https://doi.org/10.3390/su15119060